AD-A053 263　NAVAL SURFACE WEAPONS CENTER WHITE OAK LAB　SILVER SP--ETC　F/G 11/6
ELASTIC VERSUS MAGNETOELASTIC ANISOTROPY IN RARE EARTH-IRON ALL--ETC(U)
NOV 77　J R CULLEN, S RINALDI, G V BLESSING
UNCLASSIFIED　　　NSWC/WOL/TR77-180　　　　　　　　　　　　NL

1 OF 1
AD
A053263

END
DATE
FILMED
6-78
DDC

AD A 053263

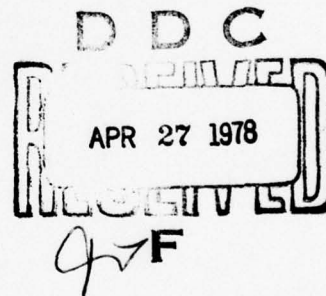# ELASTIC VERSUS MAGNETOELASTIC ANISOTROPY IN RARE EARTH-IRON ALLOYS

BY J. R. CULLEN
    S. RINALDI
    G. V. BLESSING

DDC
RECEIVED
APR 27 1978

AD No.
DDC FILE COPY

NAVAL SURFACE WEAPONS CENTER

Dahlgren, Virginia 22448 • Silver Spring, Maryland 20910

SECURITY CLASSIFICATION OF THIS PAGE (When Data Entered)

REPORT DOCUMENTATION PAGE	READ INSTRUCTIONS BEFORE COMPLETING FORM
1. REPORT NUMBER NSWC/WOL TR77-180 2. GOVT ACCESSION NO.	3. RECIPIENT'S CATALOG NUMBER
4. TITLE (and Subtitle) ELASTIC VERSUS MAGNETOELASTIC ANISOTROPY IN RARE EARTH-IRON ALLOYS	5. TYPE OF REPORT & PERIOD COVERED Summary Report 11/1/76 - 11/1/77
	6. PERFORMING ORG. REPORT NUMBER
7. AUTHOR(s) J.R. Cullen, S. Rinaldi, G.V. Blessing	8. CONTRACT OR GRANT NUMBER(s) N0001477WR 70090
9. PERFORMING ORGANIZATION NAME AND ADDRESS Naval Surface Weapons Center White Oak Laboratory White Oak, Silver Spring, Maryland 20910	10. PROGRAM ELEMENT PROJECT, TASK AREA & WORK UNIT NUMBERS 61153N; RR011-08; RR011-08-01; NR384-916;
11. CONTROLLING OFFICE NAME AND ADDRESS RR011 08	12. REPORT DATE 1 Nov 1977
	13. NUMBER OF PAGES 30 35 p.
14. MONITORING AGENCY NAME & ADDRESS(if different from Controlling Office) RR0110801	15. SECURITY CLASS. (of this report) Unclassified
	15a. DECLASSIFICATION/DOWNGRADING SCHEDULE

16. DISTRIBUTION STATEMENT (of this Report)

Approved for public release; Distribution unlimited.

17. DISTRIBUTION STATEMENT (of the abstract entered in Block 20, if different from Report)

DDC
APR 27 1978
F

18. SUPPLEMENTARY NOTES

To be published in the Journal of Applied Physics, March 1978.

19. KEY WORDS (Continue on reverse side if necessary and identify by block number)

Rare Earth Compounds
Magetostrictive Materials
Elastic Constants

20. ABSTRACT (Continue on reverse side if necessary and identify by block number)

A review is presented of recent results of ultrasonic investigations of rare earth-iron compounds and alloys. The discussion is divided into three sections. The first describes results of sound velocity measurements of single crystal $Tb_{.3}Dy_{.7}Fe_2$ as a function of magnetic field strength and orientation with respect to the crystallographic axes. In the second part recent work on polycrystalline and amorphous samples, including evidence for simultaneous propagation of two different types of magnetoelastic waves is presented. A model developed to describe this phenomenon is outlined as well

DD FORM 1473 EDITION OF 1 NOV 65 IS OBSOLETE
1 JAN 73
S/N 0102-LF-014-6601

over

SECURITY CLASSIFICATION OF THIS PAGE (When Data Entered)

391 596

(20) Finally a transmission experiment in a single crystal ($Tb_{.3}DY_{.7}Fe_2$) is described. Resonant-like transmission is shown to take place when an applied magnetic field is so oriented as to produce almost equal velocities for C_{44} and $C_{11}-C_{12}$ modes.
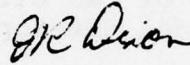
SUMMARY

A review is presented of recent results of ultrasonic
investigations of rare earth-iron compounds and alloys. The discussion
is divided into three sections. The first describes results of sound
velocity measurements of single crystal $Tb_{.3}Dy_{.7}Fe_2$ as a
function of magnetic field strength and orientation with respect
to the crystallographic axes. In the second part recent work on
polycrystalline and amorphous samples, including evidence for simul-
taneous propagation of two different types of magnetoelastic waves
is presented. A model developed to describe this phenomenon is
outlined as well.

Finally a transmission experiment in a single crystal ($Tb_{.3}Dy_{.7}Fe_2$)
is described. Resonant-like transmission is shown to take place
when an applied magnetic field is so oriented as to produce almost
equal velocities for the C_{44} and $C_{11}-C_{12}$ modes.

PREFACE

The work reported here represents a portion of the research
carried out by the Magnetism and Materials Group, Solid State Branch,
Research and Technology Department, to determine the elastic proper-
ties of highly magnetostrictive rare earth-iron alloys. The work
was supported by the Office of Naval Research (Task No. RR011-08-01).
The report summarizes results on single crystal, polycrystalline
and amorphous alloys.

J. R. DIXON
By direction

CONTENTS

ILLUSTRATIONS

4

ILLUSTRATIONS (CONT)

TABLES

INTRODUCTION

Magnetically ordered solids generally undergo a change in length relative to their length in the demagnetized condition. This relative length change, or magnetostriction is an intrinsic property of the magnet and varies in size from nearly one percent in ferromagnetic Rare Earth metals at low temperatures to a few parts in a million in the ferromagnetic transition elements Co, Fe and Ni. [1] Magnetostriction results from the coupling of the magnetic moments to the lattice distortions. This same interaction is capable of modifying the elastic properties of magnetostrictive materials. Besides the changes in modulus brought on by domain-wall movements such as the ΔE effect [2], there are often measurable changes in the elastic properties in magnetically saturated materials. The latter effects are most clearly observable in single-crystal specimens. Changes in elastic constants are most pronounced in highly magnetostrictive magnets. In Ni for example, changes in elastic constants of the order of 10^{-3} have been observed [3]; in rare earth metals these changes can be several percent [4].

1.   Clark, A. E., in Handbook of the Physics and Chemistry of the Rare Earths, K. Gschneidner and H. Eyring, eds. North Holland (Amsterdam), to be published.

2.   Bozorth, R. M., Ferromagnetism, Van Nostrand 1951.

3.   Alers, G. A., Neighbours, J. R., and Sato, H., J. Phys, Chem. Solids 9, 21 (1958).

4.   Moran, T. J., and Luthi, B., J. Phys. Chem. Solids 31, 1735 (1970).
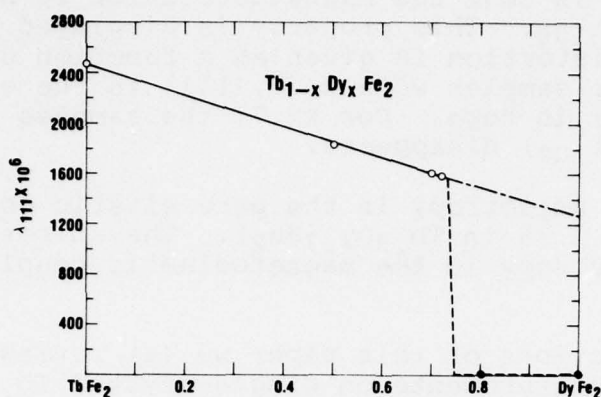
Fig. 1   Magnetostriction constant λ_{111} determined by the
x-ray method.

For ferromagnets, an estimate for the change in elastic constant
can be made from the formula

$$\delta C/C = -\lambda^2 C/K. \tag{1}$$

Here C is a modulus, λ the magnetostriction and K the magnetic
anisotropy. For Ni, C $\simeq 10^{12}$erg/cm^3, K $\sim 10^5$ erg/cm^3, $\lambda \sim 10^{-5}$ and
Equation (1) gives $\delta C/C \sim 10^{-3}$. That the changes in modulus are so
dependent on magnetic anisotropy simply reflects the fact that the
slowing of a sound wave is accomplished by a rotation of the moment.

Recently, attempts have been made to produce materials which
would have the high magnetostriction characteristic of the rare earths
but have this property available at room temperature. Success was
achieved [1] with the cubic rare earth-iron compounds RFe$_2$, where
R stands for a rare earth element. In TbFe$_2$ for example,
$\lambda_{111} \simeq 2.6 \times 10^{-3}$ at room temperature. Since this is two orders
of magnitude larger than the magnetostriction in Ni, we would expect
modulus changes of several percent in these compounds were it not
for their characteristically large magnetic anisotropy. The latter
difficulty can be overcome with little expense in magnetostriction,
however, by forming pseudobinary compounds R$_{1-x}$R'$_x$ Fe$_2$ with a
suitable choice of x. In Tb$_{.3}$Dy$_{.7}$Fe$_2$, for instance K is less than
10^6 erg/cm^3 while λ is still large (1.6×10^{-3}). The reason this
tailoring of λ and K works is that these two quantities depend almost
exclusively on the rare earth constituent. Using these two values,
the formula gives $\delta C/C \simeq -1$ at room temperature. This was more than
ample motivation for an ultrasonic investigation of the elastic
constants of this type of pseudobinary compound.

7

One other characteristic property of these compounds is of special interest here. That is that the magnetostriction is highly anisotropic: $\lambda_{111} >> \lambda_{100}$. This property is displayed in Figure 1 in which the x-ray distortion is given as a function of x in $Tb_{1-x}Dy_xFe_2$. [5] For samples with x<.7, [111] is the easy axis and the distortion (λ_{111}) is huge. For x>.7, the samples have [100] easy and the distortion (λ_{100}) disappears.

We expect little anisotropy in the pure elastic constants (a ≡ 2 $C_{44}/C_{11}-C_{12}$ ≃ 1.25 in $Tb_{.3}Dy_{.7}Fe_2$). The anisotropy in λ then translates into anisotropy in the magnetoelastic coupling: $b_2 >> b_1$.

In succeeding sections of this paper we (a) review our recent ultrasonic velocity measurements on single-crystal $Tb_{.3}Dy_{.7}Fe_2$ from which the elastic constants and b_2 were determined; (b) discuss recent results of velocity measurements in highly magnetostrictive poly-crystalline and amorphous rare earth-iron alloys. Finally, we describe a measurement on single-crystal $Tb_{.3}Dy_{.7}Fe_2$ of a resonant coupling of the C_{44} mode to the $C_{11}-C_{12}$ mode which is a direct consequence of the anisotropy in magnetostriction and the fact that $\delta C/C > a-1$.

SINGLE CRYSTAL RESULTS: C_{44} and $C_{11}-C_{12}$

The velocity of transverse sound waves was measured in a single crystal of $Tb_{.3}Dy_{.7}Fe_2$. [6] The direction of propagation was [110]. All our measurements were done at room temperature, using frequencies near 10 MHz. Figure 2 shows the results of applying a magnetic field of up to 25 kOe in various directions for both [001] (C_{44}) and [1$\bar{1}$0] ($C_{11}-C_{12}$) polarizations of the sound. Note that the velocity of [001] waves has been reduced by thirty percent upon rotating the field in the (110) plane from perpendicular to the polarization to parallel to it. This corresponds to more than a 50 percent reduction in C_{44} as we anticipated from the estimate given above. The velocity of the $C_{11}-C_{12}$ waves was increased by a percent or so as the magnetic field was rotated from perpendicular to the polarization to parallel to it. From the form of the magnetoelastic energy in terms of the magnetization components M_i and the strains ϵ_{ij} for cubic systems, ie. we see that b_2 couples components of the moment to C_{44}-type

$$E_{me} = \frac{b_1}{M_s^2} \Sigma_i (M_i^2-1/3)\epsilon_{ii} + \frac{b_2}{M_s^2} \Sigma_{i \neq j} M_iM_j\epsilon_{ij} \qquad (2)$$

5. Clark, A., Cullen, J., McMasters, O., and Callen, E., A.I.P. Conf. Proc. No. 29, (A.I.P. New York) p. 129.

6. Rinaldi, S., Cullen, J. R., and Blessing, G. V., Phys. Lett. 61A, 465 (1977).
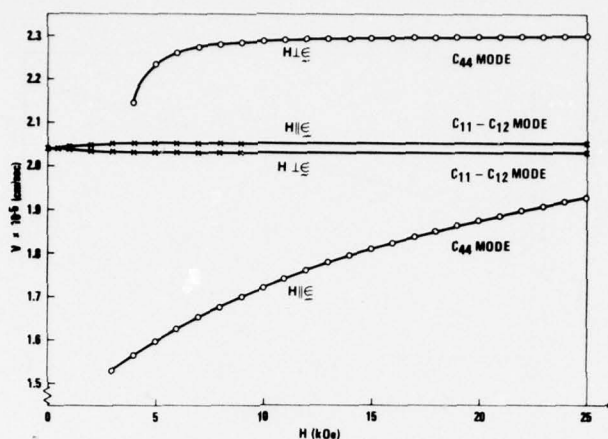
Fig. 2 Sound velocity vs. magnetic field: polarizations along
[001] (circles) and along [110] (crosses). For each
polarization, data for two orientations of field are shown.

(ε_{ij} $i \neq j$) strains while b_1 is appropriate for C_{11}-C_{12} (ε_{ii}-ε_{jj})
strains. Thus the large changes in C_{44} and relatively small ones in
C_{11}-C_{12} confirm the results of earlier work that $b_2 >> b_1$.

From Equation (2) and the quasi-static approximation [7], which
is good whenever the sonic frequencies are much less than the ferro-
magnetic resonance frequency, it is possible to calculate the change
in the elastic energy in terms of the susceptibility tensor and the
components of the moment and magnetic field. For H // [001] the
change in C_{44} is predicted to be (H^O is the total internal field,)

$$C_{44} = C_{44}^O - b_2^2/(H+H^O)M_S \qquad (3)$$

i.e. the sum of the anisotropy field and $4\pi M_S$ in the case of
conducting materials like these.

Here C_{44}^O is the pure elastic constant. The change in C_{44} for
$H//[1\bar{1}0]$ is zero; thus $C_{44}(H//[1\bar{1}0]) = C_{44}^O$ and by plotting
$(C_{44} - C_{44}^O)^{-1}$ vs. H, $|b_2|$ was determined from the slope of the
resulting straight-line portion (see Figure 3) to be 2.3×10^9 erg/cm^3
in excellent agreement with earlier measurements. [1]

7. See for example, Le Craw, R. C., and Comstock, R. L., in
Physical Acoustics ed. W. Mason Vol III B page 127 (Academic
Press 1965).

9
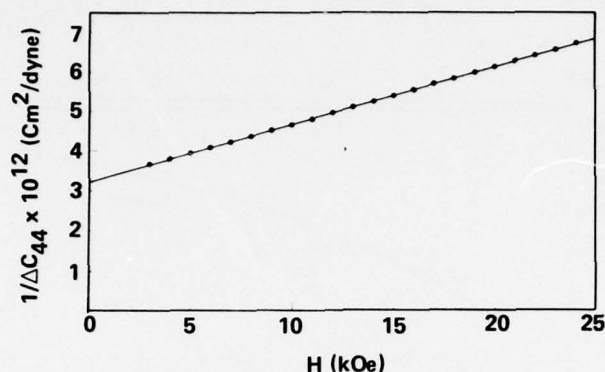
Fig. 3 The reciprocal of the difference in C_{44}, $(C_{44}^O-C_{44})^{-1}$ plotted vs. magnetic field. b_2 is determined from the slope.

Further verification of the magnetostrictive origin was obtained from a plot of (Cmax-C)/(Cmax-Cmin) versus the angle of the magnetic field with respect to the crystalline axes (Figure 4). The high-field limit of the theory [8] based on (2) is the solid line in this figure. We see that the over-all agreement is quite good, better at 10 kOe than at 6 kOe. This is understandable considering that the theoretical curve is a high-field limit. Returning to the $(C_{44}^O-C_{44})^{-1}$ vs. H plot, from the intercept and (3) we obtained the magnetic anisotropy. Using 800 Oe for M_S we found K= 4 x 10^6 erg/cm^3, about eight times greater than the value obtained from more conventional methods. [9]

We mentioned that the velocity of the $C_{11}-C_{12}$ type mode actually increased slightly when according to (2), it should have decreased (see Figure 5). This is evidence for a non-linear term in the magnetoelastic coupling. Since the shift in $C_{11}-C_{12}$ is independent of applied field, the non-linear coupling [10] is probably the "morphic" type, [11]

$$E'_{me} = F M_i M_j \epsilon_{kl} \epsilon_{mn} \tag{4}$$

8. Simon, G., Naturf, Z., 13A 84 (1958).

9. Williams, C., and Koon, N., Conference on the Rare Earths and Actinides, J. Phys. (to be published).

10. Bonsall, L., and Melcher, R., Phys. Rev. 14, 1128 (1976); Dohm, V., and Fulde, P., Z. Phys. B21, 368 (1975).

11. Mason, W., Phys. Rev. 82, 715 (1951).

where F is a tensor of rank six. We will return to this question
of non-linearity in the final section.
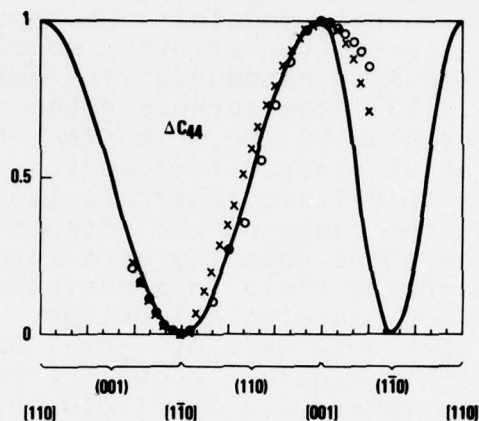
Fig. 4 Angular variation of the relative change: $(C_{max}-C)/(C_{max}-C_{min})$
in elastic constant (C_{44}) in the (001), (110) and $(1\bar{1}0)$ planes.
Circles: 6 kOe data. Crosses: 10 kOe. The full lines
are a result of linear magnetoelastic theory.
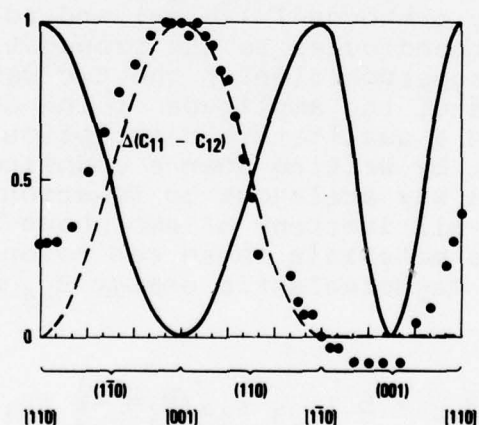
Fig. 5 Angular variation of the relative change: $(C_{max}-C)/(C_{max}-C_{min})$
in elastic constant $(C_{11} - C_{12})$ in the $(1\bar{1}0)$, (110) and (001)
planes. All data taken at 10 kOe. Dashed lines correspond
to the morphic effect; full lines correspond to linear
magnetoelastic theory.

11

POLYCRYSTALLINE AND AMORPHOUS MATERIALS: ELASTIC ISOTROPY

Changes in moduli in magnetostrictive polycrystalline materials are very often observed and usually attributed [2] to the movement of domains. Changes in Young's modulus were reported earlier at low fields [12] in rare earth-iron alloys. Modulus changes in a series of polycrystalline RFe_2 compounds were measured at 10 MHZ in fields up to 25 kOe. [13] The authors noted that in $TbFe_2$ saturation was not achieved even at 25 kOe. The fact that such large changes were observed at ultrasonic frequencies, too high for domain walls to follow, led us to believe that rotation of the magnetization by the strain field was the cause of the effects. We therefore made [14] a study of the sound velocity as a function of the magnitude and orientation of a magnetic field in a series of highly magnetostrictive polycrystals with low magnetic anisotropy. Included in the study, besides $Tb_{.3}Dy_{.7}Fe_2$ were $Sm_{.88}Dy_{.12}Fe_2$, $Sm_{.7}Ho_{.3}Fe_2$ and amorphous $TbFe_2$ (a-$TbFe_2$). Figure 6 shows the pattern of echoes we observed from a-$TbFe_2$ taken with the field at various angles θ with respect to the direction of polarization of the transducer. For $\theta = 0^O$ or 90° we observed a single train of echoes, though those at 0° were delayed relative to those at 90°. At intermediate θ, however, we observed a superposition of the 0° and 90° patterns indicating that two shear waves are propagating simultaneously, with different velocity, in these configurations. It is clear from Figure 6 that the height of the shorter-time pulse (amplitude of the faster wave) decreases as θ decreases from 90°, while the delayed-pulse height (slow-wave amplitude) increases. We checked our interpretation of the double echo pattern by making a through transmission experiment with the transmitter and receiver shear polarizations mutually orthogonal ($\varepsilon_T \perp \varepsilon_R$) and rotating the magnetic field in the plane perpendicular to the propagation. Using a large pulse width to allow superposition of the two waves, the expected $\sin \theta \cos \theta$ dependence of the amplitude of the detected signal was verified. We obtained a qualitative description of the two waves simultaneously present by writing down a coupling between strain and magnetization in a way analagous to Equation (2), but taking into account the over-all isotropy of amorphous and polycrystalline matter. For isotropic materials there can be only one coupling constant b, since the magnetoelastic energy E_{me} must be rotationally invariant. Thus

$$\overline{E}_{me} = b \sum_{i,j} \varepsilon_{ij}(\overline{M}_i \overline{M}_j - \frac{1}{3} \delta_{ij}) \tag{5}$$

12. Savage, H., Clark, A., and Powers, J., IEEE Trans. Mag. MAG-11, 1355.

13. Klimker, H., Rosen, M., Dariel, M. P., and Atzmony, U., Phys. Rev. B10, 2968 (1974).

14. Blessing, G., Cullen, J., and Rinaldi, S., to be published.

12
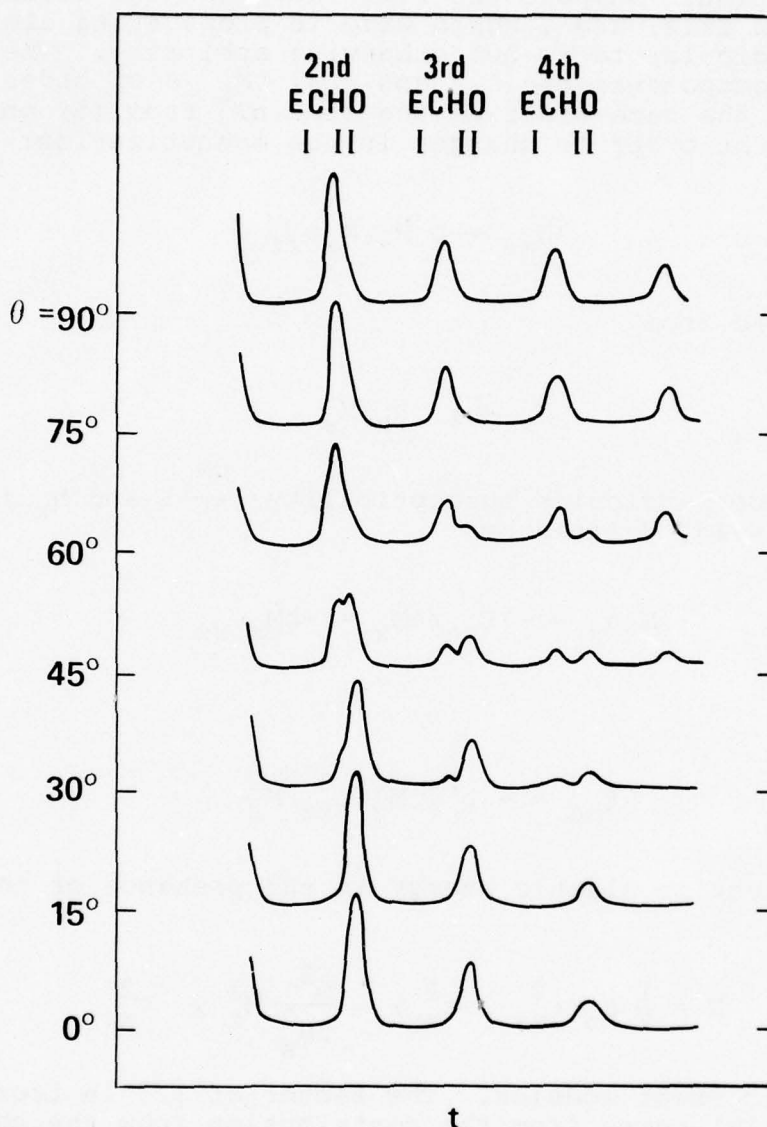
Fig. 6   Observed echo pattern for shear waves propagating perpendi-
cular to the applied field H in amorphous TbFe2. The
changes in the amplitudes of the peaks as the angle θ between
the direction of H and the direction of polarization is
varied indicate the presence of two normal modes with
polarization parallel and perpendicular to H. The positions
of the peaks do not change, indicating that there is no
variation in the velocity of the normal modes.

The $\bar{M}_i$ are the components of the average magnetization normalized to one at saturation. Suppose the field and thus the average moment to be along the z axis, and a sound wave is propagating along x, polarized perpendicular to x, but otherwise arbitrary. The only non-zero strain components are ε_{xy} and ε_{xz}. $\bar{M}_z$ is of order one; $\bar{M}_x$ and $\bar{M}_y$ are of the same order as the strain. From (5) only ε_{xz} is coupled in first order to changes in the magnetization:

$$\bar{E}_{me} \simeq b \, \bar{M}_z \, \bar{M}_x \varepsilon_{xz} \tag{6}$$

$\bar{M}_x$ can be obtained from

$$\bar{M}_x = \chi \quad h_x / M_s \tag{7}$$

where χ is the perpendicular susceptibility $(\dfrac{dM_x}{dh_x})$ and h_x is the magnetoelastic field, defined by

$$M_s h_x = -\partial \bar{E}_{me} / \partial \bar{M}_x = -b \bar{M}_z \varepsilon_{xz} \tag{8}$$

Thus

$$\bar{E}_{me} = - b^2 \chi \, \bar{M}_z^2 \, \varepsilon_{xz}^2 / M_s^2 \tag{9}$$

The total increment in elastic energy in the presence of the sound wave is then

$$\bar{E} = \frac{1}{2} \mu_o (\varepsilon_{xz}^2 + \varepsilon_{xy}^2) - \frac{b^2}{2M_s^2} \bar{M}_z^2 \chi \quad \varepsilon_{xz}^2 \tag{10}$$

μ_o is the elastic shear modulus. The factor of 1/2 in front of the second term in (10) comes from the contribution from the change in magnetic energy, which is $-1/2 \, E_{me}$. From (10) we see that the degeneracy of the shear modes is broken. The normal modes are waves, linearly polarized along the z and y axes, i.e., parallel and perpendicular to the field. These conclusions moreover do not depend for their validity on the simplified model just presented. Because of elastic isotopy in the plane perpendicular to the propagation only the magnetic field picks out a special direction, and we expect the normal modes to be polarized either parallel or perpendicular to the field. This principle applies to any elastically isotropic system in the presence of a magnetic field; the size of the splitting is proportional to the square of the magnetoelastic coupling. Since b is close to $b_2/2$, which, as we mentioned at the outset is two orders of magnitude larger than the coupling in any other room-temperature

14

magnet, it is not surprising that this effect has never been reported before in polycrystals. The same effect of course can take place in single crystals if the propagation is for example parallel to a [100] direction in a cubic crystal. Again, elastic isotropy of the (100) plane can be broken by a field in this plane. This effect, magnetoacoustic birefringence, was predicted [15] essentially using Equation (3), and has been observed in single crystals of Ni and Fe_3O_4 [16]. In [16], velocity differences of the order of 10^{-3} were measured using a phase-sensitive technique. We have observed relative changes ($\Delta v/v$) of twenty-six percent in $Sm_{.7}Ho_{.3}Fe_2$ (Table 1).

Magnetic field dependences of both velocities were separately measured to 25 kOe. Results are plotted for all four samples in Figure 7. The splitting into two waves was clearly observable to fields of 25 kOe, the largest available.
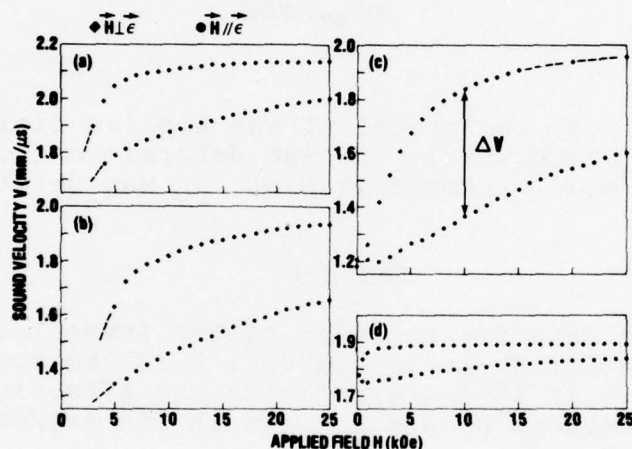
Fig. 7   Velocity as a function of applied field for $\vec{H} \perp \vec{\epsilon}$ and $\vec{H}//\vec{\epsilon}$ in
(a) $Tb_{.3}Dy_{.7}Fe_2$, (b) $Sm_{.88}Dy_{.12}Fe_2$, (c) $Sm_{.7}Ho_{.3}Fe_2$, and
(d) a-$TbFe_2$.

The velocities of the slow modes could not be saturated even at 25 kOe; the velocity of the fast mode of a -$TbFe_2$ is apparently saturated above 2 kOe (Figure 7d). The fast modes of the polycrystals, especially the compounds containing Sm show significant field dependencies to 25 kOe. By plotting the modulus of the fast modes versus l/H we obtained the pure elastic modulus μ_o from the extrapolation l/H → 0 (Figure 8). The values so obtained are listed in

15. Kittel, C., Phys. Rev. 110, 836 (1958).

16. Lüthi, B., Appl. Phys. 8, 107 (1966).

Table 1. Then, from the slopes of $(\mu_o-\mu)^{-1}$ vs. H plots (Figure 9), we obtained a pair of coupling parameters $b_{//}$ and b for the slow and fast modes respectively for each sample. These are also given in Table 1.
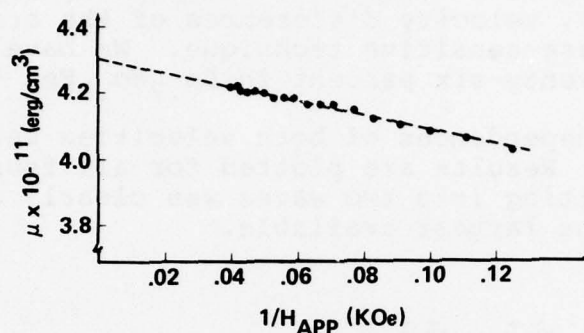
Fig. 8 Modulus (μ) vs. reciprocal of the applied field for $Tb_{.3}Dy_{.7}Fe_2$ polycrystal. μ was determined from the velocity of the fast mode. From this plot, μ_o was determined.

TABLE 1

Elastic and magnetic data for the RFe_2 alloys investigated. The saturation magnetization M_S is in emu/cm^3; V is the sound velocity; elastic modulus μ_o is in 10^{11} erg/cm^3; and the effective magneto-elastic coupling constants b and $b_{//}$ are in 10^9 erg/cm^3.

RFe_2 Alloy	M_S	$(\frac{\Delta V}{V})_{max}$	μ_o	b	$b_{//}$	$(\frac{\Delta V}{V})$
$Tb_{.3}Dy_{.7}Fe_2$	780	0.13	4.3	0.13	1.3	0.01
$Sm_{.88}Dy_{.12}Fe_2$	360	0.21	3.4	0.47	1.4	0.11
$Sm_{.7}Ho_{.3}Fe_2$	145	0.26	3.5	0.35	0.9	0.15
$a-TbFe_2$	390	0.06	2.9	0.07	0.5	0.02
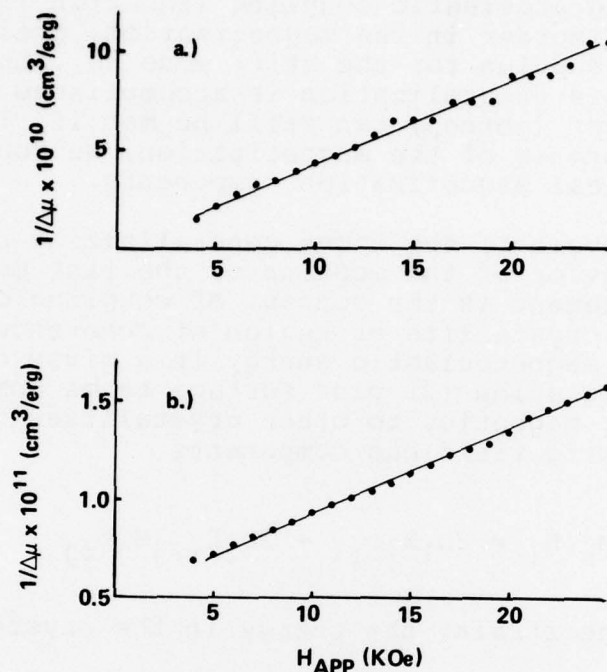
Fig. 9 Reciprocal of the difference of the modulus from the pure
elastic modulus ($\mu-\mu_o$) vs. magnetic field for $Tb_{.3}Dy_{.7}Fe_2$.
From the slopes the b's were determined. a) soft mode,
b) stiff mode.

As far as the slow ($\vec{H} || \vec{\epsilon}$) modes are concerned, the simple model
outlined above describes the data fairly well. Since for large H,
$\chi \simeq M_s/H$, Equation (10) predicts for the change in modulus $\delta\mu_{//}$ of
the slow mode

$$\delta \mu_{//} = - b^2_{//}/M_s H \tag{11}$$

Equation (11) correctly gives the large H behavior of the slow mode.
It also predicts that the modulus changes are larger, for a given b,
for samples with smaller saturation magnetization, in agreement with
the facts; the largest reduction in modulus occurs in $Sm_{.7}Ho_{.3}Fe_2$,
which has the lowest M_s (Table 1). (Table 1 also shows that the
b's are roughly the same for all the polycrystals.)

17

On the other hand, the model is inadequate for a description of the field dependence of the fast mode. A generalization, based again on isotropic magnetoelastic coupling (Equation (5)) but taking some account of the disorder in the magnetization, predicts that there is a change in modulus for the stiff mode $\delta\mu$, but going as $1/H^3$ for large H. This generalization is accomplished by recognizing that the requirement of isotropy can still be met if, instead of averages of the components of the magnetization, we couple the strains to products of the local magnetization components.

Although an improvement, the above generalization cannot reproduce the observed $1/H$ behavior of the modulus of the fast modes. The key to further improvement is the concept of coupling on a local scale, i.e. for each crystallite or region of coherence in the amorphous case. The magnetoelastic energy in a given cubic crystallite is just Equation (2) plus surface terms coming from couplings, elastic or magnetic, to other crystallites or regions. The local magnetoelastic field has components

$$M_s h_i = 2b_1 M_i \epsilon_{ii} + 2b_2 \Sigma_{i\neq j} M_j \epsilon_{ij} \tag{12}$$

To second order in the strain, the energy in the crystallite is lowered by

$$\delta E = -\frac{1}{2} \Sigma_{i,j} h_i X_{ij} h_j \tag{13}$$

The h_i are components of a real vector only when $b_1=b_2$; in general their value depends on the set of axes defining them. Thus even if the magnetization and the strain were uniform the h_i would vary from crystallite to crystallite. The material has its total energy lowered by the interaction (Equation (13)) at the expense of inducing a disorder in the magnetization. Therefore at very high magnetic fields, in the presence of a strain there are fluctuating components of the magnetization in the plane perpendicular to the net magnetization direction; these in turn will couple to the strain components in this plane. This is the mechanism which leads to a $1/H$ dependence of the modulus of the stiff mode.

The arguments given above should hold true even if there are interactions between the grains or local regions, just as long as these do not completely inhibit the creation of magnetization fluctuations via the magnetoelastic interaction. For the limiting case of independent crystallites it is possible to calculate the change in modulus of either mode at high fields. Assuming a uniform distribution of crystallite axes, δE (Equation (13)) is averaged

over the unit sphere for a set of fixed strains. The results for
the changes in shear moduli are

$$\delta\mu_\perp \simeq -\frac{8}{105}\frac{(b_2-b_1)^2}{HM_s} \equiv -\frac{b_\perp^2}{HM_s} \tag{14}$$

for polarization perpendicular to the field (stiff mode) and

$$\delta\mu_{//} \simeq -(1+\frac{4}{5}\frac{b_1-b_2}{b_1+b_2}+\frac{4}{15}(\frac{b_1-b_2}{b_1+b_2})^2)\frac{(b_1+b_2)^2}{HM_s} \equiv -\frac{b_{//}^2}{HM_s} \tag{15}$$

for the polarization parallel to the field (soft mode). As we
anticipated, the 1/H behavior of the fast mode depends entirely on
the anisotropy in the single crystal magnetostriction. In fact,
the approach to saturation magnetostriction was previously shown [17]
to behave in a similar way. As we mentioned in the introduction,
it is characteristic of RFe_2 materials that $\lambda_{111}>>\lambda_{100}$ ($b_2>>b_1$).

In the large anisotropy limit, i.e. $b_1 \to 0$ from (14) and (15)
the ratio of the coefficients of the 1/H law for the two modes is
predicted to be

$$(\frac{b_\perp}{b_{//}})^2_{b_2\to 0} = 0.163 \tag{16}$$

In the limit of magnetoelastic isotropy, i.e. $b_1=b_2$, the prediction
is that $b_\perp/b_{//} = 0$. The experimental values listed in Table 1 all
fall between these two extremes of the theory. From the discussion
following Equation (13) we take this to indicate the presence of
interactions between grains. However this intergranular interaction
is not strong enough to eliminate the magnetoelastic anisotropy.
Metallographic work shows that the samples containing Sm, which
according to Table 1 are closest to behaving like collections of
independent crystallites, contain appreciable amounts of intergranular
precipitates. Much finer grain boundaries were observed in the
$Tb_{.3}Dy_{.7}Fe_2$ sample.

There are aspects of this work on disordered RFe_2 materials still
to be worked out, including a description of the low field behavior
of the moduli and measurements of their temperature dependencies.
The most important result of this section and which leads us into
the next, is the breaking of the elastic isotropy by the
magnetoelastic coupling.

17. Lee, E. W., Proc. Phys. Soc. A 67, 381 (1954).

RESONANT TRANSMISSION OF SOUND IN A SINGLE CRYSTAL

Up to this point there has been a certain dichotomy in the presentation; on the one hand we described single crystal results in terms of changes in velocity of modes (C_{44}, $C_{11}-C_{12}$) of fixed polarization while on the other we interpreted polycrystalline data by means of modes of constant velocity whose polarization depended on the direction of the field. In describing the single-crystal results we have implicitly assumed that the appropriate symmetry
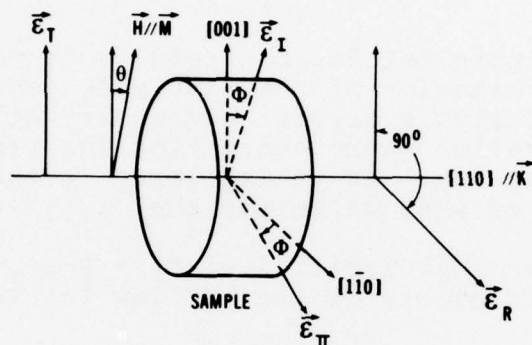
Fig. 10 Experimental arrangement for the resonance experiment in $Tb_{.3}Dy_{.7}Fe_2$ single crystal. A shear wave is generated by a transmitting transducer with polarization $\vec{\epsilon}_T$// [001] and propagates through the sample along the [110] direction. At the other side of the sample a receiving transducer with polarization $\vec{\epsilon}_R$// [1$\bar{1}$0] $\perp$ $\vec{\epsilon}_T$ detects a signal due to the rotation ϕ of the polarizations of the normal modes ($\vec{\epsilon}_I$, $\vec{\epsilon}_{II}$) induced by magnetoelastic interaction with the magnetization $\vec{M}$. The magnetization is assumed parallel to the field $\vec{H}$ applied in the (110) plane at an angle θ from the [001].

for elastic modes was determined by the crystal. Clearly there is some competition between the crystalline symmetry and that induced by the magnetic field via the magnetoelastic coupling. Generally the latter is taken to be a perturbation of the former [3,8], so that the directions of polarization of the transverse modes are only slightly tilted by an angle ϕ from the crystalline axes for any orientation θ of the magnetic field with respect to the [001] axis. (See Figure 10). This tilting of the polarization is predicted to occur only if both b_2 and b_1 (Equation (1)) are non-zero. In fact a straightforward but lengthy calculation of the velocities and

directions of polarization of the normal modes can be carried out;
[8, 18] the resulting equations for the velocities $v_{\pm}$ are:

$$v_{\pm}^2 = \frac{C+C'}{2} \pm \left(\left(\frac{C-C'}{2}\right)^2 + B^2 \right)^{\frac{1}{2}} \qquad (17)$$

The parameters C, C' and B are:

$$C \equiv C_{44}^{O}/\rho - b_2^2 \cos^2\theta \; / \; (H+H^O)M_s\rho \qquad (18)$$

$$C' \equiv (C_{11}-C_{12})^O/2\rho - b_1^2 \sin^2\theta \; / \; (H+H^O)M_s\rho \qquad (19)$$

$$B \equiv b_1 b_2 \sin\theta\cos\theta \; / \; (H+H^O)M_s\rho \qquad (20)$$

where ρ is the density.

If B=0 (θ=0 or 90°) there are two transverse waves polarized
along [001] and [1$\bar{1}$0] with velocities $C^{1/2}$ and $C'^{1/2}$ respectively;
though either C or C' is reduced (depending on whether θ = 0 or 90°)
by the magnetoelastic coupling, they are nonetheless "pure" modes
in that they are polarized along crystalline axes. In general we
only expect strong effects if C$\simeq$C' assuming b_1 and $b_2 \neq 0$. We know
from just looking at the curves of Figure (2) that this will happen
for some $\theta=\theta_c$ in Tb$_{.3}$Dy$_{.7}$Fe$_2$ because C<C' for θ=0 but C>C' for
θ=90°. (θ is measured with respect to [001]). Furthermore, $b_1 \ll b_2$
in RFe$_2$ compounds so the range of θ around θ_c where strong coupling
can take place is small. We have plotted v versus θ in Figure (11)
using known values of b_2, M_s, C_{44}, $C_{11}-C_{12}$ and H_O and taking
$b_1 \simeq 0.1 b_2$, H=8 kOe. To see what happens to the polarization
direction under these conditions, we calculated ϕ from

$$\tan\phi_{\pm} = \frac{B}{(C'-C)/2 \pm ((C'-C)^2/4 + B^2)^{\frac{1}{2}}} \qquad (21)$$

ϕ is very close to 0 or 90° except in the immediate vicinity of θ_c
where it changes abruptly.

To check this "pulling" of the axes of polarization off the
crystalline axes we performed a transmission experiment (Figure (10))
in which receiving and transmitting transducers were arranged with
linear polarization along crystallographic axis and orthogonal to
one another. A magnetic field of 8 kOe was rotated in the (110)
plane, and the output of the receiver recorded. We expect this
output to vary as A sin 2ϕ, where A is another oscillatory function
of θ coming from interference. Using the same set of parameters
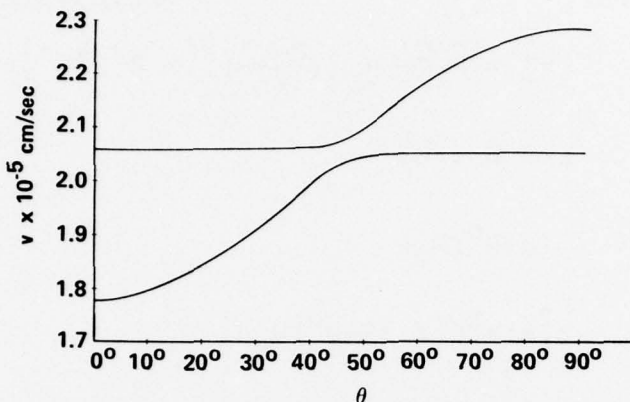listed above, we have calculated the expected amplitude as a function

Fig. 11   Dispersion in the velocity of the shear normal modes for
[110] propagation in $Tb_{.3}Dy_{.7}Fe_2$ caused by the interaction
of the strain with the magnetic moment in the (110) plane
at an angle θ from the [001]. The parameters used are:
$b_1 = 2 \times 10^8$ erg/cm^3; $b_2 = 2.3 \times 10^9$ erg/cm^3; $(C_{11}-C_{12})/$
$2 = 3.9 \times 10^{11}$ erg/cm^3; $C_{44} = 4.8 \times 10^{11}$ erg/cm^3;
$M_S = 1000$ emu/cm^3; $\rho = 9.2$ g/cm^3, $H_O = 20$ kOe, $H = 8$ kOe.

of θ. The result is plotted in Figure (12a). The envelope, peaked
around 45°, is due to sin 2ϕ while the oscillations come from A.
We have also plotted a modified version of the amplitude obtained
by correcting Figure (12a) for depolarization and finite resolution:
Figure (12b). The experimental results are given in Figure (12c).
There is reasonably good agreement, i.e. the theory reproduces the
sharp central peak and much of the structure away from the crossover
angle. Although this agreement verifies our picture of the rotation
of the polarization, the theoretical model must still be made
consistent with our earlier discussion of Figure (2) in which we
pointed out that the slight stiffening of the $C_{11}-C_{12}$ mode was
inconsistent with Equation (2). Including non linear terms of the
form of Equation (4) means simply replacing $b_1^2/M_S(H+H_O)$ by itself
plus f_1 and $b_1b_2/M_S(H+H_O)$ by itself plus f_2 in Equation (19) and
(20) [18]. f_1 must be negative and larger in magnitude than
$b_1^2/M_S(H+H_O)$ to explain the stiffening of $C_{11}-C_{12}$. Since the relative
change in $C_{11}-C_{12}$ is about 2%, f_1 must be about 10^{10} erg/cm^3. Now
the width of the central peak in the transmission amplitude is best
fit by choosing $b_1b_2/M_S(H+H_O) + f_2 \simeq 10^{11}$ erg/cm^3. If $|f_1| \simeq |f_2|$ it
must be the combination b_1b_2 that is responsible for coupling the

18.   Rinaldi, S., and Cullen, J., to be published.

INFINITE RESOLUTION

5 10 15 20 25 30 35 40 45 50 55 60 65 70 75 80 85

RESOLUTION = ± 2°

5 10 15 20 25 30 35 40 45 50 55 60 65 70 75 80 85

EXPERIMENT: Tb.3 Dy.2 Fe2

5 10 15 20 25 30 35 40 45 50 55 60 65 70 75 80 85

$\theta \longrightarrow$
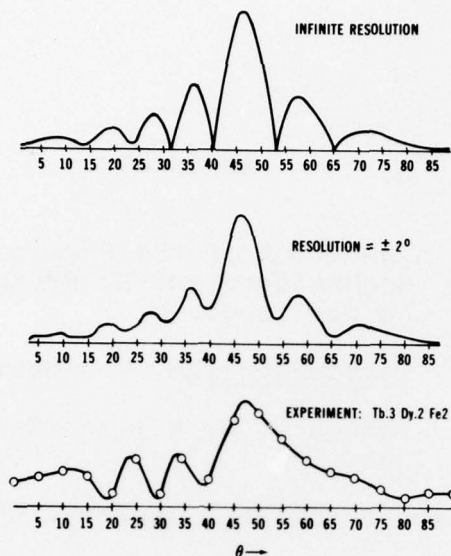
Fig. 12 Comparison between the theoretical prediction and the experimental results of the resonance experiment described in the text and in Figure 10. The parameters used for the theoretical curves are the same as in Figure 11.

two transverse modes. At this stage of our knowledge, we can only regard these estimates as tentative.

The expectation of large changes in elastic properties of RFe_2 compounds due to moment rotations has been amply justified. The measurements described here have further shown that the elastic isotropy of polycrystalline and amorphous RFe_2 alloys is removed in a magnetic field and that the elastic anisotropy of crystalline compounds can be nullified and even inverted. Most of the observed effects are accounted for by linear magnetoelastic theory if $b_2 \gg b_1$ and proper account of the fluctuation in magnetization is taken. Discrepancies indicate the presence of non linear magnetoelastic interactions.

REFERENCES

1. Clark, A. E., in Handbook of the Physics and Chemistry of the Rare Earths, K. Gschneidner and H. Eyring, eds. North Holland (Amsterdam), to be published.

2. Bozorth, R. M., Ferromagnetism, Van Nostrand 1951.

3. Alers, G. A., Neighbours, J. R., and Sato, H., J. Phys, Chem. Solids 9, 21 (1958).

4. Moran, T. J., and Luthi, B., J. Phys. Chem. Solids 31, 1735 (1970).

5. Clark, A., Cullen, J., McMasters, O., and Callen, E., A.I.P. Conf. Proc. No. 29, (A.I.P. New York) p. 129.

6. Rinaldi, S., Cullen, J. R., and Blessing, G. V., Phys. Lett. 61A, 465 (1977).

7. See for example, Le Craw, R. C., and Comstock, R. L., in Physical Acoustics ed. W. Mason Vol III B page 127 (Academic Press 1965).

8. Simon, G., Naturf, Z., 13A 84 (1958).

9. Williams, C., and Koon, N., Conference on the Rare Earths and Actinides, J. Phys. (to be published).

10. Bonsall, L., and Melcher, R., Phys. Rev. 14, 1128 (1976); Dohm, V., and Fulde, P., Z. Phys. B21, 368 (1975).

11. Mason, W., Phys. Rev. 82, 715 (1951).

12. Savage, H., Clark, A., and Powers, J., IEEE Trans. Mag. MAG-11, 1355.

13. Klimker, H., Rosen, M., Dariel, M. P., and Atzmony, U., Phys. Rev. B10, 2968 (1974).

14. Blessing, G., Cullen, J., and Rinaldi, S., to be published.

15. Kittel, C., Phys. Rev. 110, 836 (1958).

REFERENCES (CONT.)

16. Luthi, B., Appl. Phys. $\underline{8}$, 107 (1966).

17. Lee, E. W., Proc. Phys. Soc. A $\underline{67}$, 381 (1954).

18. Rinaldi, S., and Cullen, J., to be published.

DISTRIBUTION LIST

Director Defense Advanced Research Projects Agency Attn: Technical Library 1400 Wilson Blvd. Arlington, Virginia 22209	3
Office of Naval Research Physics Program Office (Code 421) 800 North Quincy Street Arlington, Virginia 22217	3
Office of Naval Research Assistant Chief for Technology (Code 200) 800 North Quincy Street Arlington, Virginia 22217	
Office of Naval Research Code 715LD (ONR/London) 800 North Quincy Street Arlington, Virginia 22217	6
Naval Research Laboratory Department of the Navy Attn: Technical Library Washington, D. C. 20375	3
Office of the Director of Defense Research and Engineering Information Office Library Branch The Pentagon Washington, D. C. 20301	3
U. S. Army Research Office Box 12211 Research Triangle Park No. Carolina 27709	2
Defense Documentation Center Cameron Station (TC) Alexandria, Virginia 22314	12
Director, National Bureau of Standards Attn: Technical Library Washington, D. C. 20234	

Commanding Officer   3
Office of Naval Research Branch Office
536 South Clark Street
Chicago, Illinois 60605

Commanding Officer   3
Office of Naval Research Branch Office
1030 East Green Street
Pasadena, California 91101

San Francisco Area Office   3
Office of Naval Research
One Hallidie Plaza
Suite 601
San Francisco, California 94102

Commanding Officer   3
Office of Naval Research Branch Office
495 Summer Street
Boston, Massachusetts 02210

New York Area Office
Office of Naval Research
715 Broadway, 5th Floor
New York, New York 10003

Director
U. S. Army Engineering Research
  and Development Laboratories
Attn: Technical Documents Center
Fort Belvoir, Virginia 22060

ODDR&E Advisory Group on Electron Devices   3
201 Varick Street
New York, New York 10014

Air Force Office of Scientific Research
Department of the Air Force
Bolling AFB, D. C. 22209

Air Force Weapons Laboratory
Technical Library
Kirtland Air Force Base
Albuquerque, New Mexico 87117

Air Force Avionics Laboratory
Air Force Systems Command
Technical Library
Wright-Patterson Air Force Base
Dayton, Ohio 45433

Lawrence Livermore Laboratory
Attn: Dr. W. F. Krupke
University of California
P. O. Box 808
Livermore, California 94550

Harry Diamond Laboratories
Technical Library
2800 Powder Mill Road
Adelphi, MD 20783

Naval Air Development Center
Attn: Technical Library
Johnsville
Warminster, Pennsylvania 18974

Naval Weapons Center
Technical Library (Code 753)
China Lake, California 93555

Naval Training Equipment Center
Technical Library
Orlando, Florida 32813

Naval Underwater Systems Center
Technical Library
New London, Connecticut 06320

Commandant of the Marine Corps
Scientific Advisor (Code RD-1)
Washington, D. C. 20380

Naval Ordnance Station
Technical Library
Indian Head, Maryland 20640

Naval Postgraduate School
Technical Library (Code 0212)
Monterey, California 93940

Naval Missile Center
Technical Library (Code 5632.2)
Point Mugu, California 93010

Naval Ordnance Station
Technical Library
Louisville, Kentucky 40214

Commanding Officer
Naval Ocean Research & Development Activity
Technical Library
NSTL Station, Mississippi 39529

Naval Explosive Ordnance Disposal Facility
Technical Library
Indian Head, Maryland 20640

Naval Ocean Systems Center
Technical Library
San Diego, California 92152

Naval Sea Systems Command
Attn: SEA-03B
Washington, D. C. 20360

Office of Chief of Naval Operations
Operations Evaluation Group (OP 03EG)
Washington, D. C. 20350

Naval Ship Research and Development Center
Central Library (Code L42 and L43)
Bethesda, Maryland 20084

Naval Avionics Facility
Technical Library
Indianapolis, Indiana 46218